ELSEVIER

Journal of Nuclear Materials 264 (1999) 133–140

journal of nuclear materials

Electronic ion energy loss calculations on the basis of the binary encounter approximation

C.A. Ordonez [a,*], D.R. Bickel [a], V.C. Venezia [a], F.D. McDaniel [a], S.E. Matteson [a], M.I. Molina [b]

[a] *Department of Physics, University of North Texas, P.O. Box 305370, Denton, TX 76203-0368, USA*
[b] *Departamento de Fisica, Facultad de Ciencias, Universidad de Chile, Santiago, Chile*

Received 27 March 1997; accepted 26 June 1998

Abstract

Electronic ion energy loss calculations on the basis of the binary encounter approximation are presented for protons in oxygen, nitrogen and silicon. Calculations using both an analytical approach as well as a Monte Carlo approach are found to agree well with experimental data even down to energies below the stopping cross section maximum. Energy loss calculations for protons in silicon under channeling conditions are included and predictions are made for channeling in the $\langle 1\,1\,0\rangle$ direction at low energies (5–500 keV).

1. Introduction

Theoretical advances in the description of fast-particle energy loss rates are of fundamental importance for improving the basic understanding of a variety of ion–solid interactions such as plasma–ion sputtering and ion implantation [1,2]. The energy loss rate experienced by fast particles as they traverse a medium is commonly characterized by the stopping power of the medium. Stopping power theory has been developed to a large extent considering fast-particle transport through a plasma of free target particles. Theoretical approaches which have been used include the collective dielectric response of the medium [3], kinetic equations [4–7], and the binary encounter approximation [8–10]. Although collective dielectric response calculations of the stopping power can be fairly accurate within a limited range of fast-particle energies (e.g. for protons above the stopping power maximum), normally, it is not simultaneously accurate (within, say, 10%) above, at, and below the stopping cross section maximum [3]. Kinetic equation approaches, which include use of the Fokker–Planck [4,5], Lenard–Balescu and Boltzmann equations [6,7] have primarily been used for describing charged-particle transport processes in non-degenerate plasmas. Use of the binary encounter approximation for evaluating stopping powers is discussed from a historical perspective in Ref. [8]. An important improvement in using the binary encounter approximation for evaluating the stopping power of a medium has been to include the velocity distribution of particles in the medium [9,10]. The present work represents an extension of these and other existing binary encounter approximation works referenced below as applied to calculating electronic ion energy loss rates about the stopping cross section maximum.

The binary encounter approximation provides a relatively simple approach for evaluating the average energy loss, δE, experienced by a point particle, a projectile, while traveling a path length, δl, through a system of non-interacting, point, target particles. Specifically, a many-body interaction is modeled as a progression of binary interactions. (A detailed discussion of this simplification is given in Ref. [11].) It is convenient to use the energy loss and path length for defining the stopping power, $\mathrm{d}E/\mathrm{d}l$, and the energy loss rate, $\mathrm{d}E/\mathrm{d}t$. The definitions are needed below. They are

$$\frac{\mathrm{d}E}{\mathrm{d}t} = \frac{\delta E}{\delta t}, \tag{1}$$

* Corresponding author.

0022-3115/99/$ – see front matter
PII: S0022-3115(98)00479-6

$$\frac{dE}{dl} = \frac{\delta E}{\delta l}. \tag{2}$$

Here, $\delta t = \delta l / v_1$, is the time it takes the projectile to travel the path length, δl at an average speed, v_1.

The rest of this paper consists of the following. In Section 2, two different relations used in prior work for the stopping power of a system of non-interacting target particles are derived simultaneously in order to show their previously unrecognized similarity. The fundamental assumptions which lead to their differences are described and discussed. In Section 3, a derivation for a new binary-encounter stopping cross section is given and comparisons between the developed theory, existing theory, and experimental data are shown. In Section 4, a new Monte Carlo approach for calculating the stopping cross section is presented. The Monte Carlo approach represents an improvement over the analytical approach in the way that binary energy transfers are taken into account. Concluding remarks are found in Section 5.

2. Energy loss to a system of non-interacting target particles

Defining an 'encounter' cross section as $\sigma_{\max} = \pi b_{\max}^2$, a projectile is considered to experience energy transfer with a target particle only when their separation becomes smaller than $b_{\max}$. Suppose the target particles form a homogeneous and isotropic distribution within configuration space with all target particles at rest. Since all encounters with target particles are assumed to occur successively, the energy loss, δE, experienced by the projectile can be written as

$$\delta E = N \frac{1}{N} \sum_{i=1}^{N} \Delta E_i = N \langle \Delta E(b) \rangle_b, \tag{3}$$

where ΔE_i is the energy transfer associated with the ith encounter, N the number of encounters the projectile experiences while traveling a path length δl, and $\langle \Delta E \rangle$ the average energy transfer per encounter. The binary energy transfer, ΔE, which occurs between the projectile and a target particle at rest depends on the impact parameter, b, of the encounter. For clarity, the subscript on the average is used to indicate which parameter is averaged over. Defining a sphere of radius, $b_{\max}$, centered at the projectile, N equals the number of target particles which pass through the forward surface of the sphere as a result of the forward motion of the projectile over a path length, δl. Thus, $N = n\sigma_{\max}\delta l$, where n is the density of target particles, and, in terms of the time length, $\delta t = \delta l / v_1$,

$$N = \delta t \, n \sigma_{\max} \, v_1. \tag{4}$$

Consequently, with Eq. (3), the energy loss is

$$\delta E = \delta t \, n \sigma_{\max} v_1 \, \langle \Delta E(b) \rangle_b. \tag{5}$$

Now suppose that all target particles have the same velocity, $\mathbf{v}_2$. In this case, the number of encounters the projectile experiences is evaluated in the rest frame of the target particles and then a transformation is made to the laboratory frame of reference. In terms of the relative speed, $u = |\mathbf{v}_1 - \mathbf{v}_2|$, between the projectile and the target particles, the number of encounters experienced by the projectile during a time, δt, in the laboratory frame is

$$N = \delta t \, n \sigma_{\max} u. \tag{6}$$

The energy loss per encounter is now written as an explicit function of the target-particle velocity in order to indicate $\mathbf{v}_2$ is not zero:

$$\delta E = N \langle \Delta E(\mathbf{v}_2, b) \rangle_b. \tag{7}$$

With Eqs. (6) and (7), the energy loss is

$$\delta E = \delta t \, n \sigma_{\max} u \, \langle \Delta E(\mathbf{v}_2, b) \rangle_b. \tag{8}$$

If a differential group of target particles in the system have the same velocity, $\mathbf{v}_2$, and these target particles are uniformly distributed with density, dn, the differential number of encounters the projectile experiences with these target particles during a time, δt, is, according to Eq. (6), $dN = \delta t dn \sigma_{\max} u$. With the target-particle velocity distribution function, $f(\mathbf{v}_2)$, normalized to unity, $dn = n d^3 v_2 f(\mathbf{v}_2)$, and with Eq. (7),

$$\begin{aligned} dE &= dN \, \langle \Delta E(\mathbf{v}_2, b) \rangle_b \\ &= \delta t \, n \, d^3 v_2 f(\mathbf{v}_2) \sigma_{\max} u \, \langle \Delta E(\mathbf{v}_2, b) \rangle_b. \end{aligned} \tag{9}$$

The total energy loss of the projectile during a time, δt, is evaluated by integrating over three-dimensional velocity space,

$$\begin{aligned} \delta E &= \delta t \, n \, \sigma_{\max} \int d^3 v_2 f(\mathbf{v}_2) \, u \langle \Delta E(\mathbf{v}_2, b) \rangle_b \\ &= \delta t \, n \, \sigma_{\max} \, \langle u \langle \Delta E(\mathbf{v}_2, b) \rangle_b \rangle_{\mathbf{v}_2}. \end{aligned} \tag{10}$$

Dividing through by δl, utilizing $v_1 = \delta l / \delta t$, and using Eq. (2) provides

$$\frac{dE}{dl} = n \, \sigma_{\max} \left\langle \frac{u}{v_1} \langle \Delta E(\mathbf{v}_2, b) \rangle_b \right\rangle_{\mathbf{v}_2}. \tag{11}$$

For all of the above, the target particles are assumed to have a homogeneous and isotropic distribution in configuration space. This assumption is now removed and, instead, a homogeneous and isotropic distribution of fixed, spherically-symmetric potential wells in configuration space is considered. Within each potential well, a single target particle is locally bound. When the projectile passes through a potential well, the projectile is assumed to have sufficient energy so that the background potential which forms the potential well has a negligible effect on its motion. It is assumed that, as the separation between the projectile and a target particle decreases to less than $b_{\max}$ and an encounter occurs, the

interaction between the projectile and the target particle is dominant. The velocity of a target particle at the instant its separation from the projectile decreases to $b_{\max}$ is, $\mathbf{v}_2$, the target-particle velocity going into the binary encounter. Evaluation of the differential number of encounters associated with target particles having velocity, $\mathbf{v}_2$, is complicated because $\mathrm{d}N$ depends on the "width" of each potential well within which each target particle is confined. First, the width of each potential well shall be considered to be much smaller than $b_{\max}$. Thus, defining a sphere of radius, $b_{\max}$, centered at the projectile, $\mathrm{d}N$ equals the differential number of potential wells, each containing a target particle, which pass through the sphere as the projectile travels a path length, δl. Since the potential wells are at rest, Eq. (4) provides the differential number of encounters associated with target particles having velocity, $\mathbf{v_2}$: $\mathrm{d}N = \delta t\, \mathrm{d}n\, \sigma_{\max} v_1 = \delta t\, n\, \sigma_{\max} v_1 \mathrm{d}^3 v_2 f(\mathbf{v}_2)$. Since the width of each potential well is considered to be much smaller than $b_{\max}$, the inhomogeneity in the spacial probability density of target particles is statistically accounted for in the evaluation of $\mathrm{d}N$ and Eq. (7) continues to apply. Using Eq. (7) provides

$$\delta E = \delta t\, n\, \sigma_{\max} v_1 \langle \Delta E(\mathbf{v}_2, b)\rangle_{\mathbf{v}_2, b}. \tag{12}$$

Dividing through by δl, utilizing $v_1 = \delta l/\delta t$, and using Eq. (2) provides

$$\frac{\mathrm{d}E}{\mathrm{d}l} = n\, \sigma_{\max} \langle \Delta E(\mathbf{v}_2, b)\rangle_{\mathbf{v}_2, b}. \tag{13}$$

Eq. (11) was used in Ref. [9] while Eq. (13) was used (without giving a derivation) in Refs. [12,13]. Eq. (13) provides a step toward taking into account (on the basis of the binary encounter approximation) the fact that certain target particles do not have a homogeneous spacial distribution. These target particles include bound electrons in solids as well as electrons forming gas atoms and molecules (with the speeds of binding nuclei assumed much smaller than the projectile speed). Unfortunately, generalization to potential well widths of arbitrary size is a formidable problem and does not appear possible. Thus, for stopping power calculations based on the binary encounter approximation, this leaves Eq. (11) which considers free target particles and Eq. (13) which takes into account a spatial inhomogeneity by considering the target particles to be trapped in fixed spacial regions which are much smaller than the encounter cross section.

Eqs. (11) and (13) are to be applied to each electron component of a target. (Here, 'electron component' refers to specific groups of electons in the target. For an elemental target of atomic number Z_2, the total electronic stopping power is the summation of stopping power contributions from Z_2 electron components). Eqs. (11) and (13) are equivalently written as stopping cross sections, $S = n^{-1}\mathrm{d}E/\mathrm{d}l$. They are

$$S = \int \mathrm{d}^3 v_2 f(\mathbf{v}_2) \frac{u}{v_1} \int \mathrm{d}\sigma\, \Delta E, \tag{14}$$

$$S = \int \mathrm{d}^3 v_2 f(\mathbf{v}_2) \int \mathrm{d}\sigma\, \Delta E, \tag{15}$$

where $\mathrm{d}\sigma$ is the differential of the encounter cross section.

3. Binary-encounter stopping cross sections

With Eq. (14), a stopping cross section relation, referred to here as a binary-encounter stopping cross section, is derived in Ref. [9] which can be written as

$$S = \int \mathrm{d}^3 v_2 f(\mathbf{v}_2) \frac{u}{v_1} \left[\frac{m_2 \mathbf{v}_1 \cdot \mathbf{u}}{m_\mathrm{r} u^2} - \frac{m_2}{m_1} \right] S_0(u). \tag{16}$$

Here, $S_0(v_1)$ is the stopping cross section in the high velocity limit ($v_1 \gg v_2$), and $m_\mathrm{r} = m_1 m_2/(m_1 + m_2)$ is the reduced mass of the two-particle system, with m_1, the projectile mass, and m_2, the target particle mass. A binary-encounter stopping cross section can also be derived for Eq. (15). A relation for the energy transferred from a projectile to a target particle in an elastic collision is needed. It is

$$\Delta E = 2m_\mathrm{r} \left(\mathbf{v}_1 \cdot \mathbf{u} - \frac{m_\mathrm{r}}{m_1} u^2 \right) \sin^2 \left(\frac{\theta_\mathrm{c}}{2} \right) - m_\mathrm{r} |\mathbf{v}_1 \mathbf{v}_2| \sin\, \theta_\mathrm{c} \tag{17}$$

where θ_c is the center-of-mass scattering angle in the plane of the collision with values between π and $-\pi$. When Eq. (17) is substituted into Eq. (15),

$$S = m_\mathrm{r} \int \mathrm{d}^3 v_2 f(\mathbf{v}_2) \left(v_1^2 - \mathrm{v}_1 \cdot \mathbf{v}_2 - \frac{m_\mathrm{r}}{m_1} u^2 \right) \sigma^1(u) \tag{18}$$

results where

$$\sigma^1(u) = 2 \int \sin^2 \left(\frac{\theta_\mathrm{c}}{2} \right) \mathrm{d}\sigma. \tag{19}$$

Note that the last term in Eq. (17) does not appear because it vanishes when integrated over the azimuthal angle. (The differential cross section $\mathrm{d}\sigma$ is considered to have azimuthal symmetry.) In the limit, $v_1 \gg v_2$, the stopping cross section becomes

$$[S_{v_1 \gg v_2}] \equiv S_0(v_1) = \frac{m_\mathrm{r}^2 v_1^2 \sigma^1(v_1)}{m_2} = \frac{2 m_\mathrm{r}^2 v_1^2}{m_2} \int \sin^2 \left(\frac{\theta_\mathrm{c}}{2} \right) \mathrm{d}\sigma. \tag{20}$$

Substituting u for v_1 in this equation, solving for σ^1, and substituting it in Eq. (18) provides

$$S = \int \mathrm{d}^3 v_2 f(\mathbf{v}_2) \left[\frac{m_2 \mathbf{v}_1 \cdot \mathbf{u}}{m_\mathrm{r} u^2} - \frac{m_2}{m_1} \right] S_0(u) \tag{21}$$

which only differs from Eq. (16) by the factor, (u/v_1), within the velocity integral. Both relations give the same result at high projectile speeds, since if $v_1 \gg v_2$, $(u/v_1) \to 1$. Consequently, only near and below the stopping power maximum will the two results differ by an appreciable amount.

For evaluating the high-speed stopping cross section, the center-of-mass scattering angle in a non-relativistic binary Coulomb collision is used. Thus,

$$\sin^2\left(\frac{\theta_c}{2}\right) = \frac{1}{1+4b^2/r_0^2}, \tag{22}$$

where $r_0 = 2e^2Z_1/m_r u^2$ becomes $2e^2Z_1/m_r v_1^2$ for $v_1 \gg v_2$. Here, e is the magnitude of an electron's charge and Z_1 is the atomic number of the projectile. Putting Eq. (22) into Eq. (20) with $d\sigma = 2\pi b\, db$ and integrating up to a maximum impact parameter, b_{max}, gives

$$S_0(v_1) = \frac{4\pi e^4 Z_1^2}{m_2 v_1^2} \ln\left(\sqrt{1+\frac{4b_{max}^2}{r_0^2}}\right). \tag{23}$$

The only unknown parameter in this equation is b_{max}, the scale length over which the projectile passes non-adiabatically. Since the projectile speed is large, Eq. (23) can be simplified to

$$S_0(v_1) = \frac{4\pi e^4 Z_1^2}{m_2 v_1^2} \ln\left(\frac{2b_{max}}{r_0}\right). \tag{24}$$

This is, in fact, the Bethe expression for the stopping cross section in the high (but non-relativistic) velocity limit when $b_{max} = 2e^2Z_1/U$ where U is the minimum excitation energy. Using this value of b_{max}, Eq. (23) is written as

$$S_0(v_1) = \frac{4\pi e^4 Z_1^2}{m_2 v_1^2} \ln\left[\sqrt{1+\left(\frac{2m_r v_1^2}{U}\right)^2}\right]. \tag{25}$$

It is convenient to separate the target particle's velocity into parallel ($\|$) and perpendicular ($\perp$) components with respect to the direction of travel of a projectile just prior to an encounter. Doing this allows the stopping cross section to be written in terms of a double integral which can be evaluated numerically. (Hence, the asymptotic approximations performed in previous binary encounter approximation work are not used here.) Inserting Eq. (25) with $v_1 \to u$ into Eqs. (16) and (21) and rearranging provides

$$S = \frac{4\pi e^4 Z_1^2}{m_r} \int dv_{2\perp} dv_{2\|} h(v_{2\perp}, v_{2\|}) \frac{w(u)}{u^4} \times \left(v_1^2 - v_1 v_{2\|} - \frac{m_r}{m_1} u^2\right) \ln\left[\sqrt{1+\left(\frac{2m_r v_1^2}{U}\right)^2}\right], \tag{26}$$

where $w(u) = u/v_1$ corresponds to Eq. (16) while $w(u) = 1$ corresponds to Eq. (21). Here, $f(\mathbf{v}_2)d^3v_2 = h(v_{2\perp}, v_{2\|})dv_{2\perp}dv_{2\|}$ and $u = \sqrt{v_1^2 + v_{2\perp}^2 + v_{2\|}^2 - 2v_1 v_{2\|}}$. One shortcoming with Eq. (26) is that integration over negative energy transfers takes place. This is discussed in more detail in Section 4.

Eq. (26) can be evaluated provided both a minimum excitation energy and a velocity distribution function are known. For the minimum excitation energy, the relation [14], $U = (1/2)m_2\langle v_2\rangle^2$, is used where $\langle v_2\rangle$ is the mean electron speed. The velocity distribution function is needed both to evaluate the velocity integral and to evaluate the mean electron speed. The velocity distribution is determined from a fit to Hartree–Fock Compton profile values for atomic electrons provided in Ref. [15]. A fit of the form

$$J(q) = \frac{J(0)}{(1+(q/a_3)^{a_2})^{a_1}} \tag{27}$$

is used for the Compton profile with parameters a_1, a_2, and a_3 given in Table 1 for oxygen, silicon and nitrogen. The normalized, isotropic distribution function is related to the Compton profile by

$$g(v_2) = -\beta v_2 \frac{dJ(v_2)}{dv_2}, \tag{28}$$

where β is chosen to provide the normalization, $\int_0^\infty g(v_2)dv_2 = 1$, with $g(v_2)dv_2 = f(\mathbf{v}_2)d^3v_2$. Also provided in Table 1 are values for $J(0)$, the root mean square errors, ϵ_{rms}, associated with the fitting pro-

Table 1
Parameters used in the stopping cross section calculations (values in atomic units)

	1s	2s	2p	3s	3p
Oxygen					
$J(0)$	0.113	0.579	0.350		
a_1	2.37	4.79	1.24		
a_2	2.03	2.01	2.86		
a_3	6.45	1.87	1.37		
ϵ_{rms}	0.00056	0.0084	0.0053		
$\langle v_2\rangle$	6.74	1.12	2.14		
Silicon					
$J(0)$	0.0635	0.275	0.149	1.04	0.744
a_1	29.0	4.00	1.37	6.18	1.92
a_2	1.97	2.07	3.01	2.00	3.03
a_3	13.2	3.44	3.43	1.18	0.802
ϵ_{rms}	0.00027	0.00073	0.0021	0.0066	0.0069
$\langle v_2\rangle$	11.6	2.34	4.58	0.597	0.820
Nitrogen ($\alpha = 1.4$)					
$J(0)$	0.13	0.672	0.407		
a_1	2.52092	4.58492	1.22687		
a_2	2.01064	2.02361	2.92666		
a_3	5.83993	1.56547	1.17843		
ϵ_{rms}	0.0011	0.0026	0.0062		
$\langle v_2\rangle$	5.77603	0.96697	1.80922		

cedure, and the calculated mean electron speeds. A transformation of coordinates in velocity space provides $h(v_{2\perp}, v_{2\parallel})$ in terms of $g(v_2)$. It is $h(v_{2\perp}, v_{2\parallel}) = (1/2)v_{2\perp}g(\sqrt{v_{2\perp}^2 + v_{2\parallel}^2})/(v_{2\perp}^2 + v_{2\parallel}^2)$.

The results for calculations of the electronic stopping cross section for protons traveling through oxygen are shown in Fig. 1 along with experimental data from Refs. [16,17]. Excellent agreement with the experimental data is found at all energies with Eq. (26) using both expressions for $w(u)$. The result using $w(u) = u/v_1$ remains within 12% of the data while the result using $w(u) = 1$ remains within 6% of the data for the entire range in energy. The close agreement between the calculations, which use Compton profiles determined for atomic oxygen, and the experimental data, which is for molecular oxygen, appears to indicate that the speed distributions for the outer electrons must be similar for atomic and molecular oxygen.

For the stopping cross section calculations for silicon, both channeling and non-channeling conditions have been considered. For non-channeling conditions, neither the use of $w(u) = u/v_1$ nor the use of $w(u) = 1$ provided good agreement with experimental data near the stopping cross section maximum. The stopping cross section profile predicted using $w(u) = u/v_1$ compared better near and below the stopping cross section maximum where the valence band electrons contributed most to the stopping cross section while the profile predicted using $w(u) = 1$ compared slightly better at higher energies where K and L shell electrons contributed most to the stopping cross section. The best results were obtained by adding the stopping cross section contribution from the K and L shells as calculated using $w(u) = 1$ to the stopping cross section contribution from the valence electrons as calculated using $w(u) = u/v_1$. For the valence electrons the minimum excitation energy had to be fit for good agreement. The necessity of this is probably associated with the use of an inaccurate speed distribution for the valence electrons as the Hartree–Fock Compton profile used was determined for atomic silicon electrons. The minimum excitation energy used was $U_{\text{val}} = 35.7$ eV. The result of this combined calculation shows good agreement with experimental data from Ref. [18] as indicated in Fig. 2. For channeled protons in silicon, stopping cross section calculations were carried out and compared to data at higher energies. There calculations show good agreement with the peak values of transmission spectra in the $\langle 1\ 1\ 0\rangle$ direction from Ref. [19] as shown in Fig. 3. The calculations were carried out just as for the non-channeling calculations except that only 10% of the contribution from 2p electrons was included and no contribution by the 1s and 2s electrons was included. Fig. 4 shows a prediction for channeling stopping cross section values using the same calculation as in Fig. 3 but extending the results to much lower energies.

4. Monte Carlo approach

In terms of a sum over energy transfers, the stopping cross section associated with Eq. (13) is

$$S = \frac{1}{n}\frac{\mathrm{d}E}{\mathrm{d}l} = \frac{16\pi e^4 Z_1^2}{\alpha^2 m_2^2 \langle v_2\rangle^4 N}\sum_{i=1}^{N}\Delta E_i. \tag{29}$$

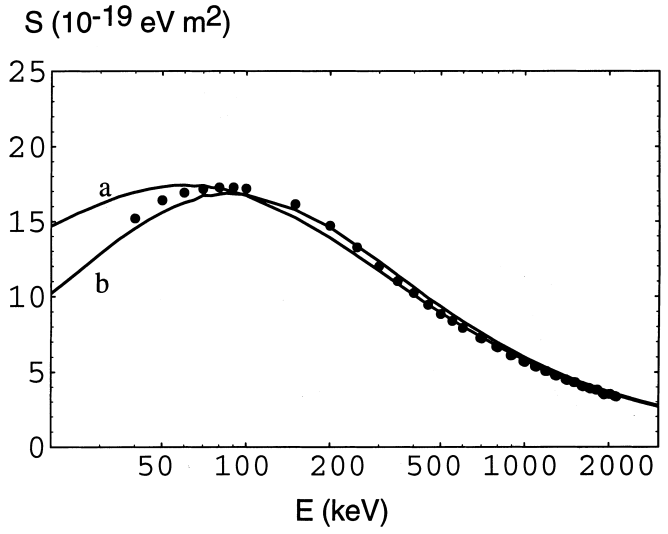

Fig. 1. Stopping cross section calculations for protons in oxygen. Shown are the results from numerical evaluations of Eq. (26) using $w = u/v_1$ (curve a) and $w = 1$ (curve b), and experimental data from Refs. [16,17].

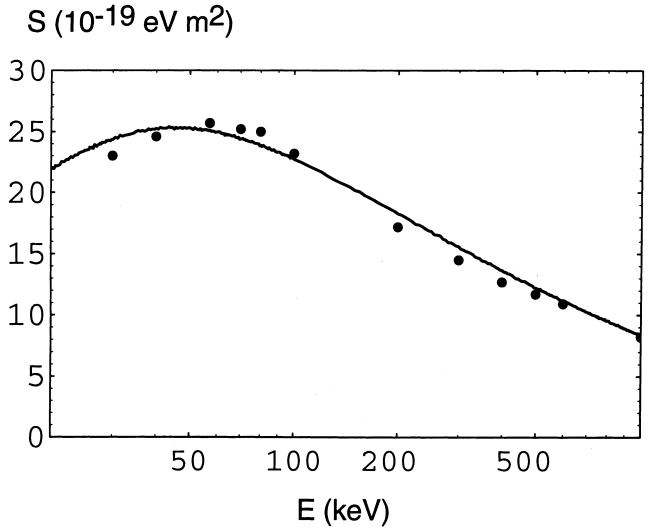

Fig. 2. Stopping cross section calculations for protons in silicon under non-channeling conditions. Interpolated experimental results are from Ref. [18].

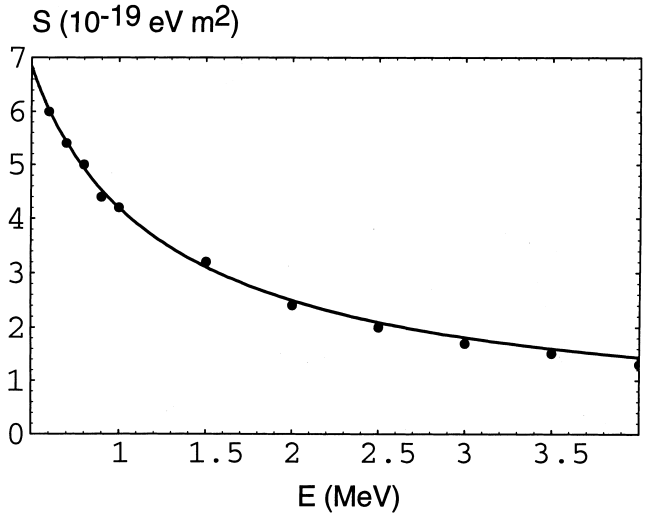

Fig. 3. Stopping cross section calculations for protons in silicon under ⟨1 1 0⟩ channeling conditions. Interpolated experimental results are from Ref. [19].

Here, $b_{\max} = 2e^2Z_1/U$, is used along with $U = \alpha(1/2)m_2\langle v_2\rangle^2$ where α is introduced as an adjustable parameter. The latter is equivalent to incorporating one fitting parameter into the calculations. This provides a means of fitting the model to experimental results in the high projectile-speed limit. From Eqs. (17) and (22), the energy transfer per collision for azimuthally-symmetric encounters is

$$\Delta E_i = \frac{2m_r(v_1^2 - v_1v_{2\|} - m_r u^2/m_1)}{1 + \sigma/\sigma_0}, \tag{30}$$

where $\sigma_0 = \pi e^4 Z_1^2/m_r^2u^4$. Hence, each energy transfer is associated with a set of values for the impact parameter cross section, σ, and the electron velocity components, $(v_{2\perp}, v_{2\|})$. To calculate these values, the impact parameter cross section and the electron speed are sampled from one-dimensional probability densities. For the impact parameter cross section, the assumption of azimuthally random encounters relative to the projectile direction of motion allows sampled values of σ to be easily generated as uniformly distributed random numbers between zero and $\sigma_{\max} = \pi b_{\max}^2$. Considering an

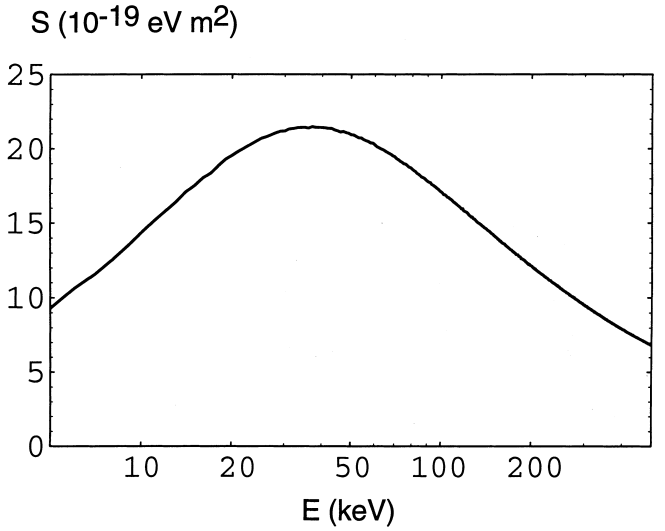

Fig. 4. Stopping cross section predictions for protons in silicon under ⟨1 1 0⟩ channeling conditions.

isotropic velocity distribution for the target electrons allows components parallel and perpendicular to the incident direction of the projectile to be generated from a sampled speed, v_2, using the relations [20], $v_{2\parallel} = v_2(1-2R)$ and $v_{2\perp} = 2v_2\sqrt{R(1-R)}$ where R is a uniformly distributed random number between zero and one. An acceptance/rejection sampling method is used to sample the electron-speed probability density, $g(v_2)$, from Eq. (28) [20].

A problem associated with the binary encounter approach is that negative values for ΔE_i can occur. Such is the case when an encountered electron travels in the direction of the projectile at a speed faster than the projectile and transfers energy to the projectile. However, assuming that target atoms are in the ground state, none of the electrons can transition down to lower lying states and give up energy to the projectile. In consideration of this, three different calculation techniques are compared. The first, and simplest, neglects the problem and includes negative ΔE_i values in the calculation. This calculation technique is the same as numerical evaluation of Eq. (26) using $w = 1$. The result of this technique is shown as curve (a) in Fig. 5. The second technique resets any negative values for ΔE_i to zero. The result of this calculation technique is shown as curve (b) in Fig. 5. Curve (b) is higher than curve (a) because the sum in Eq. (29) becomes larger as a result of replacing each negative ΔE_i by zero. In the third technique, negative values for ΔE_i are rejected in the statistical summation process. When a negative ΔE_i value is generated, the set of values, $(\sigma, v_{2\perp}, v_{2\parallel})_i$, is recalculated for the same counter, i, until a positive ΔE_i value is produced. The result of using this third technique is shown as curve (c) in Fig. 5. Curve (c) is higher than both curve (a) and curve (b) because only positive, non-zero values for ΔE_i are included in the sum in Eq. (29). Also shown in Fig. 5 is experimental data from Refs. [16,17]. The results of all three calculation techniques agree well with the experimental data and are different from each other only near and below the stopping power maximum. Of the three, the third technique provides the best agreement with the experimental data with only a slight under-prediction of the stopping power (by, at most, 6%).

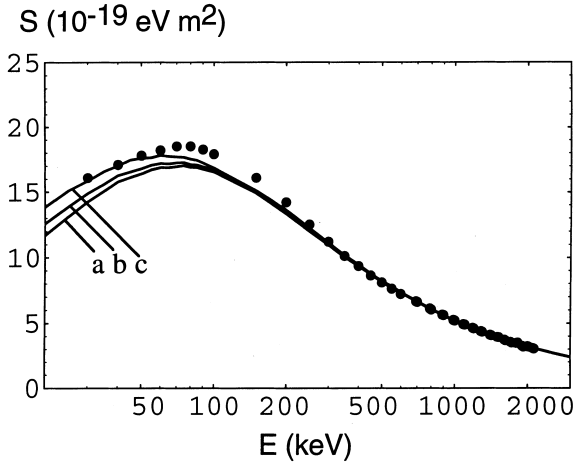

Fig. 5. The stopping cross section for protons in nitrogen. The results for calculations are shown along with experimental data [16,17]. For curve (a), numerical evaluation of Eq. (26) with $w = 1$ is used which includes integration over negative ΔE_i values. For curve (b), negative ΔE_i values are reset to zero. For curve (c), each negative ΔE_i value is recalculated and replaced by a positive ΔE_i value.

5. Conclusion

A new binary-encounter stopping cross section relation has been derived and has been used along with a previously presented binary-encounter stopping cross section relation. The fundamental difference between the two relations is the presence of a factor of u/v_1. The new binary-encounter stopping cross section relation, Eq. (21), and that previously published, Eq. (16), only depend on the stopping cross section in the limit of high projectile velocity and on the velocity distribution of the target particles. Both of the binary-encounter stopping cross sections, which were written as a single expression taking into account binary Coulomb collisions, were found to accurately provide stopping powers in oxygen (with no adjustable parameters) and in silicon (with one adjustable parameter for non-channeling conditions and two adjustable parameters for channeling conditions). For the calculations of silicon stopping cross sections, the model used agrees well with experiment at all energies in the non-channeling case and is extremely close to available experimental channeling values at energies above 500 keV. However, lower-energy experiments are needed to test the channeling predictions.

A Monte Carlo based calculation of electronic stopping cross sections has also been developed. Calculations for protons in nitrogen were presented and compared to a prediction provided by Eq. (26) and to experimental data. Of three calculation methods used, the calculation which rejects negative energy transfers (energy transfers from atomic electrons to the projectile) was found to provide the best agreement with nitrogen stopping data when α is used as a high-projectile-speed fitting parameter.

The necessity of using fitting parameters will have to be eliminated for the binary encounter approximation to represent a true theoretical (instead of semi-empirical) approach to calculating stopping cross sections. In order to refine the binary encounter approach, more accurate electron speed distributions need to be utilized for the outer electrons and an improved method of evaluating the relative probabilities associated with encountering different electron components needs to be developed.

Acknowledgements

This work was supported in part by the National Science Foundation, the Office of Naval Research, the Robert A. Welch Foundation, and a University of North Texas Junior Faculty Summer Research Fellowship.

References

[1] C.A. Ordonez, W.D. Booth, R. Carrera, M.E. Oakes, J. Nucl. Mater. 185 (1991) 130.
[2] G. Dearnaley in: R.F. Hochman, H. Solnick-Legg, K.O. Legg, Ion Implantation and Plasma Assisted Processes, ASM International, Metals Park, OH, 1988, p. 1.
[3] J.F. Ziegler, J.P. Biersack, U. Littmark, The Stopping and Range of Ions in Solids, Pergamon, New York, 1985, p. 66; and references therein.
[4] C.K. Li, R.D. Petrasso, Phys. Rev. Lett. 70 (1993) 3059.
[5] B.A. Trubnikov in: Reviews of Plasma Physics 1, Consultants Bureau, New York, 1965, p. 105.
[6] B. Strege, W.D. Kraeft, Laser Particle Beams 10 (1992) 227.
[7] W.D. Kraeft, B. Strege, Physica A 149 (1998) 313.
[8] D.R. Bates, Phys. Rep. 35 (1978) 305.
[9] P. Sigmund, Phys. Rev. A 26 (1982) 2497.
[10] E. Kührt, R. Wedell, D. Semrad, P. Bauer, Phys. Stat. Sol. B 127 (1985) 633.
[11] D.V. Sivukhin in: Reviews of Plasma Physics 4, Consultants Bureau, New York, 1966, p. 93.
[12] D. Semrad, P. Bauer, Nucl. Instr. and Meth. B 12 (1985) 24.
[13] P. Bauer, Nucl. Instr. and Meth. B 45 (1990) 673.
[14] R. Wedell, Nucl. Instr. and Meth. B 12 (1985) 17.
[15] F. Biggs, L.B. Mendelsohn, J.B. Mann, Atom. Data Nucl. Data Tables 16 (1975) 201.
[16] H.K. Reynolds, D.N.F. Dunbar, W.A. Wenzel, W. Whaling, Phys. Rev. 92 (1953) 742.
[17] G. Reiter, N. Kniest, E. Pfaff, G. Clausnitzer, Nucl. Instr. and Meth. B 44 (1990) 399.
[18] P. Mertens, P. Bauer, Nucl. Instr. and Meth. B 33 (1988) 133.
[19] J.D. Melvin, T.A. Tombrello, Radiat Effects 26 (1975) 113.
[20] I.M. Sobol, The Monte Carlo Method, University of Chicago, Chicago, 1974, p. 60.